SANDIA REPORT

SAND98–0047 • UC–706
Unlimited Release
Printed January 1998

Use of Z-Pinch Sources for High-Pressure Shock Wave Studies

C. H. Konrad, J. R. Asay, C. A. Hall, W. M. Trott, B. F. Clark, G. A. Chandler, K. G. Holland, K. J. Fleming, J. S. Lash, L. C. Chhabildas, T. G. Trucano

Prepared by
Sandia National Laboratories
Albuquerque, New Mexico 87185 and Livermore, California 94550

Sandia is a multiprogram laboratory operated by Sandia Corporation, a Lockheed Martin Company, for the United States Department of Energy under Contract DE-AC04-94AL85000.

Sandia National Laboratories

Issued by Sandia National Laboratories, operated for the United States Department of Energy by Sandia Corporation.

Available to DOE and DOE contractors from
Office of Scientific and Technical Information
P.O. Box 62
Oak Ridge, TN 37831

Prices available from (615) 576-8401, FTS 626-8401

Available to the public from
National Technical Information Service
U.S. Department of Commerce
5285 Port Royal Rd
Springfield, VA 22161

NTIS price codes
Printed copy: A04
Microfiche copy: A01

SAND98-0047
Unlimited Release
Printed January 1998

Distribution
Category UC-706

USE OF Z-PINCH SOURCES FOR HIGH-PRESSURE SHOCK WAVE STUDIES

C. H. Konrad
Shock Physics Applications Department

J. R. Asay
Shock Physics Applications Department

C. A. Hall
Shock Physics Applications Department

W. M. Trott
Energetic & Multiphase Processes Department

B. F. Clark
Pulsed Power & Laser Initiatives Department

G. A. Chandler
Diagnostics & Target Experiment Department

K. G. Holland
Shock Physics Department

K. J. Fleming
Explosive Projects Diagnostics Department

J. S. Lash
Radiographic Physics Department

L. C. Chhabildas
Shock Physics Applications Department

T. G. Trucano
Computational Physics R&D Department

Sandia National Laboratories
P.O. Box 5800
Albuquerque, NM 87185-1182

Abstract Follows

Abstract

In this paper, we will discuss the use of z-pinch sources for shock wave studies at multi-Mbar pressures. Experimental plans to use the technique for absolute shock Hugoniot measurements are discussed.

Recent developments have demonstrated the use of pulsed power techniques for producing intense radiation sources (Z pinches) for driving planar shock waves in samples with spatial dimensions significantly larger than possible with other radiation sources. Initial indications are that using Z pinch sources for producing Planckian radiation sources in secondary hohlraums can be used to drive shock waves in samples with diameters to a few millimeters and thicknesses approaching one millimeter in thickness. These dimensions provides the opportunity to measure both shock velocity and the particle velocity behind the shock front with accuracy comparable to that obtained with gun launchers. In addition, the peak hohlraum temperatures of nearly 150 eV that are now possible with Z pinch sources result in shock wave pressures approaching 45 Mbar in high impedance materials such as tungsten and 10-15 Mbar in low impedance materials such as aluminum and plastics. In this paper, we discuss the use of Z pinch sources for making accurate absolute EOS measurements in the megabar pressure range.

Contents

1. Introduction 4

2. Experimental Technique 4
- Figure 1. Photograph of the Z Accelerator 5
- Figure 2. Vacuum Hohlraur Configurations for Shock Wave Experiments 5
- Figure 3. Wire Array Used for Z-Pinch Experiments 6
- Figure 4. Hohlraum Configuration 6
- Figure 5. Hohlraum Design for Shock Wave Experiments 7
- Figure 6. Sample Configuration for EOS Experiments 8
- Figure 7. Shock Breakout Measurements Using Fiber Optics 8
- Figure 8. Effects Induced Fluorescence and Darkening in LiF and Rad-Hard 200 μm Fibers 9
- Figure 9. Fiber Configuration for Shock Breakout on the Secondary Hohlraum, S2 9
- Figure 10. Photograph of Target Configuration 10
- Figure 11. Schematic drawing of the VISAR and Fiber Optic Coupling 10

3. Numerical Simulations 10
- Figure 12. Calculated VISAR Records for Baseline Z-53 Drive from 50-300 μm Depth 11
- Figure 13. Pressures Achievable with Z-Pinch Sources as a Function of Radiation Drive Temperature 12

4. Accomplishments 12

5. References 13

6. Distribution 14

1. Introduction

There is a continuing need to determine the equation of state (EOS) and constitutive properties of materials to multi-megabar pressures in support of both weapons and non-weapons applications. Shock wave techniques have been a principal tool for determining the high pressure equation of state (EOS) of materials in regimes inaccessible by other methods (1). High-velocity launchers remain the standard tool for making these measurements. However, conventional gun technology is limited to launch velocities of about 8 km/s. Projectile impact at these velocities will produce shock pressures in materials ranging from about 1 Mbar in low-Z materials to about 7 Mbar in high-Z materials. For ultra-high EOS measurements, underground nuclear tests (2) have been used to produce shock wave pressures of about 3000 Mbar.

Existing scientific and programmatic problems, however, require EOS studies to shock pressures to tens of megabars. This requirement results in a need to increase the velocity capability of launchers to significantly higher velocities and to develop other sources of shock wave drive for high-pressure EOS studies.

Laser and pulsed power radiation sources are being explored for accessing the extremely high-pressure states of matter. For example, Evans et al. (3) have developed direct deposition laser techniques using impedance matching to produce shock waves in copper to pressures of about 20 Mbar. Most recently, Cauble et al. have developed laser back-lighting technique for making absolute measurements of the equations of state of low atomic number materials in regimes of extremely high pressure (4). Experimental loading conditions, however, pose limitations on the sample sizes possible with laser sources. This size restriction also limits the experimental possibilities for studying a broader range of material properties other than equation of state.

Pulsed power sources can also be used for planar shock wave studies and offer several potential advantages. Baumung et al. (5) are developing proton beam techniques to launch thin flyer plates to high velocities. Another approach is to use the radiation produced by imploding plasmas to produce indirect x-ray deposition on a sample. This approach has been previously explored by Fortov and coworkers (6). Recent advances in pulsed power source at Sandia National Laboratories allow use of Z pinch techniques to produce cylindrically imploding plasmas to produce black-body radiation temperatures approaching 150 eV on time scales of a few nanoseconds (7). The intense radiation source can be used to produce planar shock pressures of several tens of Mbar on the surface of a large specimens; an advantage in that it may be possible to produce uniform shock waves in samples considerably larger than characteristic of other pulsed radiation sources.

2. Experimental Technique

The overall objective of EOS experiments is to demonstrate the feasibility of obtaining accurate, absolute measurements of the shock Hugoniot for materials experiencing ablative loading. Specifically, a time resolved particle velocity must be made on a known material for comparison with previous data gathered using conventional loading techniques. Shock arrival at a surface needs to be accurately detected, and a measure of the planarity of the shock front which is traveling in the material of interest needs to be obtained.

The pulsed radiation source used for the shock wave experiments is the "Z" accelerator at Sandia, previously referred to as PBFA-Z (7). This is a 4.5 MV accelerator that uses Marx generators to store capacitive energies of about 11 MJ. In the present configuration, fast switching techniques are used to produce currents ranging up to 17 MA in thin conductive wires between a cathode and anode. An overall picture of the accelerator is shown in Figure 1 and the geometry for producing current in the wire array is shown in Figure 2. Current is generated in the cathode/anode array over a time scale of about 100 ns.

Figure 1. Photograph of the Z accelerator.

The cathode/anode arrangement shown in Figure 2 has been optimized to minimize the inductance of the systems for efficient delivery of energy to the wire array that is used to produce the Z pinch.

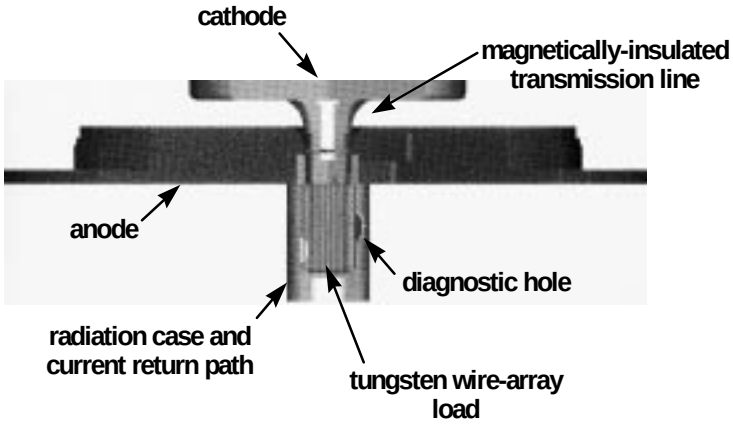

Figure 2. Vacuum hohlraum configuration for shock wave experiments

A photograph of the actual wire array is shown in Figure 3. Typically, a few hundred wires are used to produce the Z pinch source. For shock wave experiments, tungsten arrays of 120 to 240 wires of wires of about 10 μm diameter will be used to produce the Z pinch source. The diameter of the wire array itself will be 40 mm.

A photograph of a typical primary vacuum hohlraum with two secondary hohlraums attached at right angles is illustrated in Figure 4.

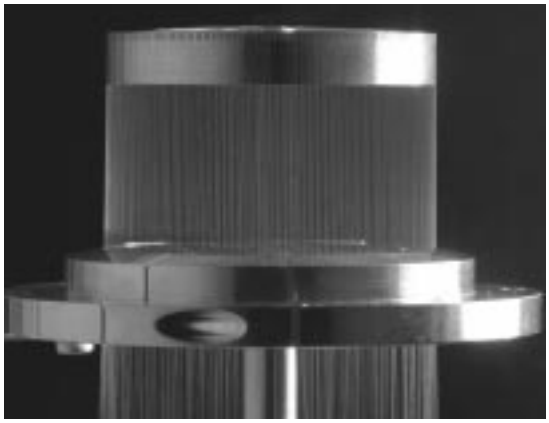

Figure 3. Wire array used for Z pinch experiments.

Typical primary hohlraum diameters are 2-5 cm with 1-2 cm heights. Also shown in Figure 4 is a typical X-ray diode (XRD) measurement of a Z pinch which is formed after implosion of the tungsten wire array on axis within the primary hohlraum. Typical pinch diameters are about 2 mm in diameter. Temperatures in the primary hohlraum can extend to nearly 150 electron volts (eV). A typical primary hohlraum temperature and secondary temperature history is illustrated in Figure 4.

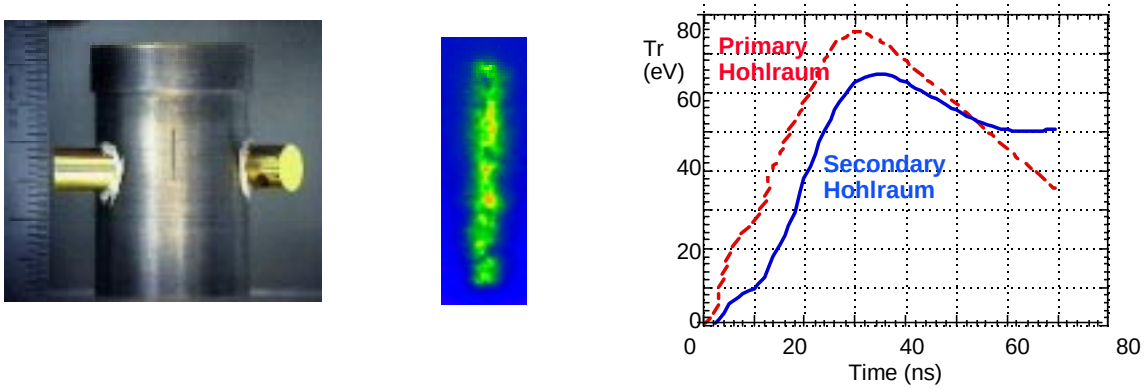

Figure 4. Hohlraum configuration and typical x-ray temperatures obtained in primary and secondary hohlraums during Z pinch experiments. An XRD measurement of a pinch after implosion is also shown.

A cross-sectional view of the hohlraum used for shock physics experiments is illustrated in Figure 5. The primary hohlraum will be about 5 cm in diameter. This will contain the radiation produced by the imploded pinch. XRD diagnostics will be used to characterize the radiation temperature history in the primary hohlraum through a Line-of-Sight (LOS 5/6) located on the Z accelerator.

Three secondary hohlraums will be attached to the primary. These will be identical, with diameters of about 11 mm OD, 9 mm ID, lengths of about 1 cm and with a small shield at the entrance to prevent direct shining of the pinch radiation onto the sample surface. Samples will be located at the end of the secondary hohlraums in general. One secondary, S1, will contain a specimen with a VISAR (8) interferometer and fiber optic shock breakout diagnostics. A second hohlraum, S2, will contain an array of fiber optics to measure shock uniformity and shock speed through a stepped aluminum sample and

also a second stepped aluminum sample that will allow another measurement of shock breakout. A third hohlraum, S3, will be capped at the end and will have a 4-mm diameter hole for XRD diagnostics to measure the temperature history through LOS 1/2. In addition a second VISAR can be utilized at this position. All inside surfaces are coated with a 10 μm thick gold coating to increase re-radiation and enhance the uniformity of the temperature fields.

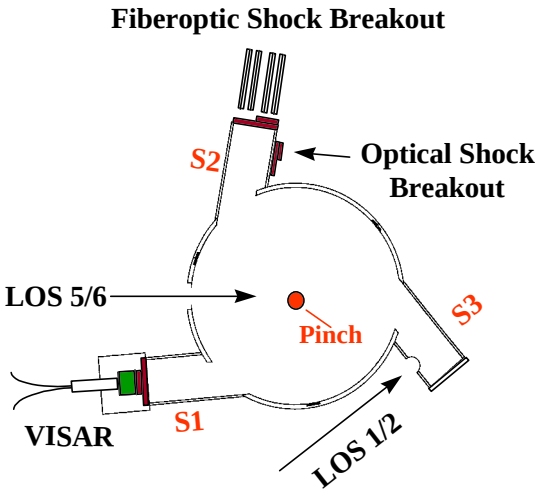

Figure 5. Hohlraum design for shock wave experiments.

The configuration being developed for the VISAR experiments is illustrated in Figure 6. The sample itself is a "hat-shaped" specimen of aluminum that will have a diameter ranging from 6-9 mm and a thickness of a few hundred micro-meters. The sample will be located on the end of the secondary hohlraum. The objective is to uniformly radiate the full input surface of the sample, causing a planar shock wave. A series of fiber optic breakout detectors will be used to measure shock arrival at the first step. A VISAR will be used to measure shock arrival at the second step and to simultaneously measure the pressure profile at that point. The combined measurements can be used to determine shock pressure and density through the shock jump conditions (1):

$$P = \rho_0 U_s u_p$$
$$\rho_0 U_s = \rho (U_s - u_p),$$

where P is the shock pressure, ρ_0 and ρ are the initial and final densities after shock compression, U_s is shock speed and u_p is particle speed. Measurement of both the shock and particle speeds allows a direct measure of pressure and density.

A miniature fiber optics probe was developed to focus the initial laser beam on the interface between the LiF window and aluminum sample and to collect the reflected diffuse light for use in the VISAR.

The ability of the fiber technique to detect shock breakout has been tested with laser driven flyers accelerated to about 3 km/s, impacting onto aluminum samples. This projectile velocity for symmetric impact produces shock pressures of about 300 kbar. A signal from one of these experiments is shown in Figure 7. The streak record on the left shows the actual intensity from the return light signal which is

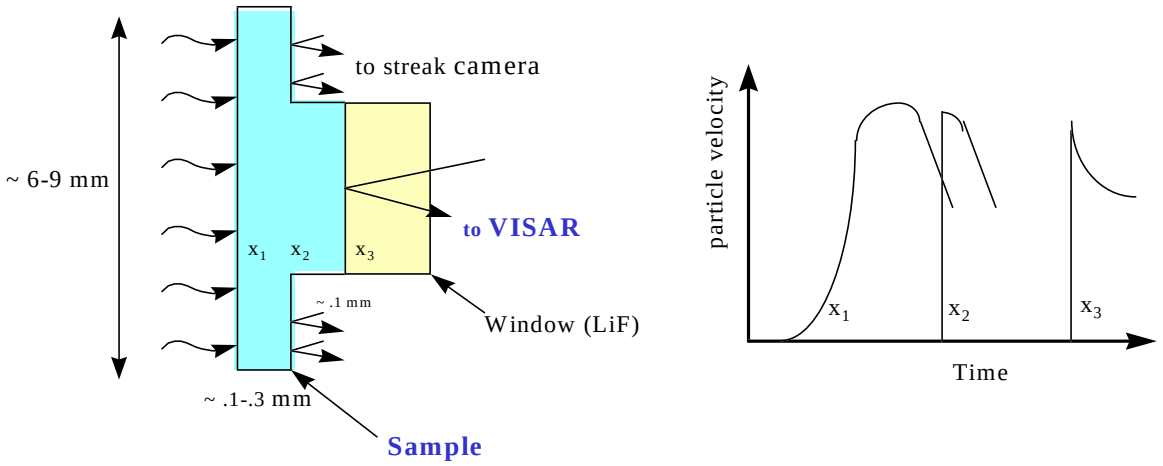

Figure 6. Sample configuration for EOS experiments.

extinguished near the middle of the record. The figure on the right shows a line out of the signal intensity, illustrating the drop in signal intensity at shock breakout. Analysis of these results indicates that the shock breakout can be detected with a time resolution of about 200 picoseconds.

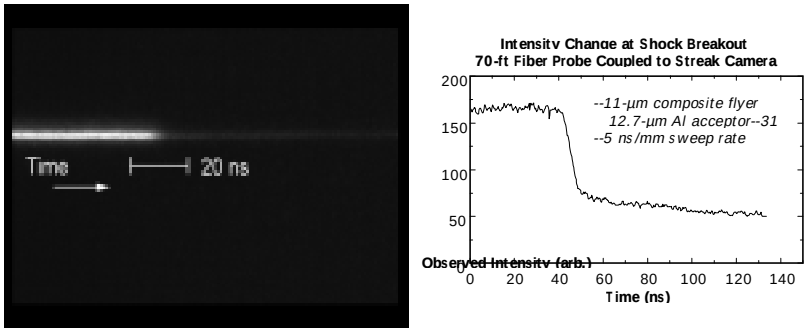

Figure 7. Shock breakout measurements using fiber optics

In addition, the optical components were tested in this environment to examine their feasibility for use. Initial experiments consisted of irradiating 200-µm core rad-hard fibers by placing them with four inches of the Z pinch load. This resulted in a fluorescence signal that routinely saturated the detectors. Fiber darkening was tested by passing an argon ion laser beam through the fiber and observing the decrease in transmission during and after radiation dose. Tests showed that the fiber initially fluoresces, then darkens nearly 100% due to the high radiation dose. However, the fluorescence signal is on the order of 10 ns FWHM, while approximately 1 µs elapses before the fiber transmission drops to zero. Thus both effects can be mitigated with filtering.

Figure 8 shows the result of an experiment on LiF in which a argon ion signal is transmitted during a Z pinch experiment. The XRD signal occurring at about 150 ns corresponds to the Z pinch signal. At this time, the LiF window darkens about 30%, but recovers over a time scale of 400 ns. The fiber does not

appreciably darken at this time, but does darken 100% at about 1 μs. Similar experiments were conducted with the micro-lens used in the probe for the VISAR experiment.

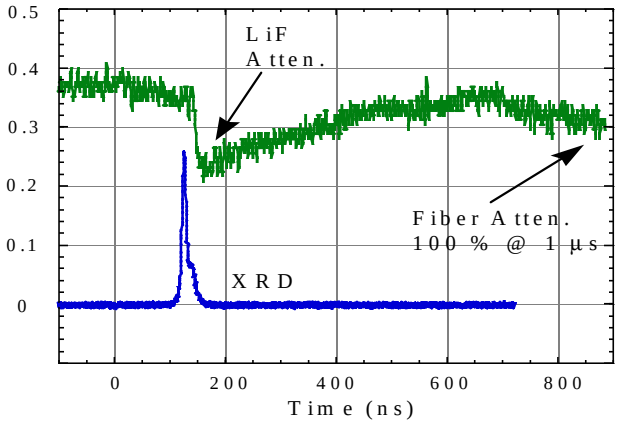

Figure 8. Effects induced fluorescence and darkening in LiF and rad-hard 200 μm fibers.

Figure 9 illustrates the placement of fiber breakout probes on the end-cap stepped aluminum plates on the secondary hohlraum, S2. Fibers have been arranged to probe spatial uniformity of loading in two orthogonal directions.

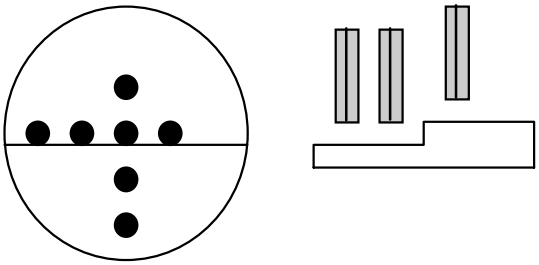

Figure 9. Fiber configuration for shock breakout on the secondary hohlraum, S2.

The VISAR optical probe assembly is illustrated in Figure 10. A central primary hohlraum is shown with a 11-mm secondary hohlraum directly viewing the pinch region and another off-axis secondary with a probe assembly mounted on it. The probe assembly has been partially machined to show the sample, the LiF window and the central optics probe with an enclosed lens. The sheathed fibers are the fiber optic breakout probes.

The secondary S3 is used for characterizing the source conditions in the secondary hohlraum. A four-channel XRD will be used to determine x-ray temperatures in the secondary. A seven-channel silicon detector will provide greater sensitivity for measuring the low energy portion of the x-ray spectrum. Finally, a time-resolved pinhole camera will be used to provide additional information about aperture size during the experiment to estimate the specific flux emitted by the secondary walls.

Figure 10. Photograph of target configuration.

A schematic diagram of the diagnostic configuration is shown in Figure 11. A modulated cw laser will be used for recording the interferometer data from the VISAR on a stepped aluminum specimen as illustrated earlier. A dye laser operating at 514.5 nm is used for the fiber optic and open beam shock breakout experiments. To minimize the effects of Bremstrahlung-induced fluorescence a 1 nm pass-band filters is used to eliminate broadband light from contaminating the optical data. All of the signals are recorded on a fast streak camera which provide time resolution of about 200 ps.

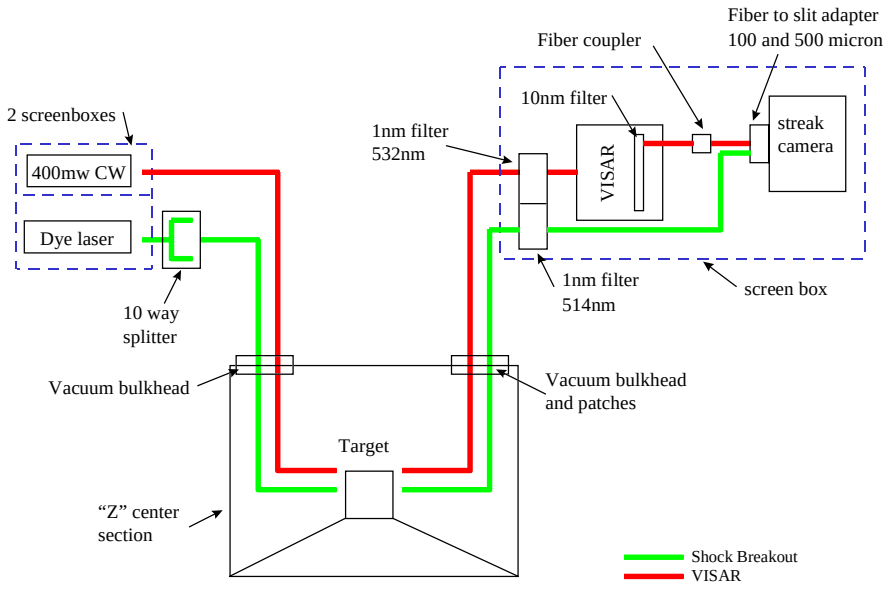

Figure 11. Schematic drawing of the VISAR and fiber optic coupling

3. Numerical Simulations

To optimize the loading conditions for producing uniform steady compression in shock wave experiments planned on Z, we simulated the ablation pressures in various materials using a 15 ns wide trapezoidal radiation source (Planckian) in the ALEGRA (9) code. This code utilizes an implementation

of the SPARTAN SPN package developed by Morel and Hall (10,11). Materials studied included CH, Al, Ti, and W, using SESAME EOS tables and opacity determined by XSN. Peak temperatures for the assumed radiation pulse were chosen over the interval of 50 to 200 eV, which is characteristic of the secondary radiation hohlraums.

Two types of calculations were undertaken. First, direct illumination of the targets was performed. Second, calculations were done with a CH ablator. For direct illumination, we found that ablation pressures increased more rapidly with peak source temperature than expected for tungsten and titanium.

The primary hohlraum drive for the experiments being planned on Z is similar to the temporal dependence of the secondary temperature history illustrated in Figure 4. Small variations were made from the records illustrated to estimate the pressure profiles expected in aluminum specimens. For a blackbody of about 100 eV and a FWHM temperature history of about 20 ns, the profiles shown in Figure 12 are expected for different propagation distances. It is noted that attenuation is minimal over the distance of 50-200 μm. At 200 μm, peak stress attenuation is minimal to at least 300 μm.

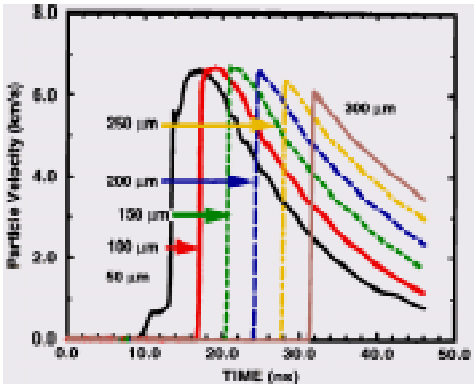

Figure 12. Calculated VISAR records for the baseline Z-53 drive, from 50-300 μm depth.

A systematic series of experiments were performed with another code, referred to as LASNEX (12), assuming a similar temporal dependence for the secondary hohlraum temperature. In this case, it was assumed that the temperature rose linearly to peak in 10 ns, remained at the peak for 10 ns, then return to zero in 10 ns. The peak pressures obtained for varying peak drive temperatures is illustrated in Figure 13. Also shown is a scaling relation (12) that has been developed to give approximate peak pressures at different peak drive temperatures.

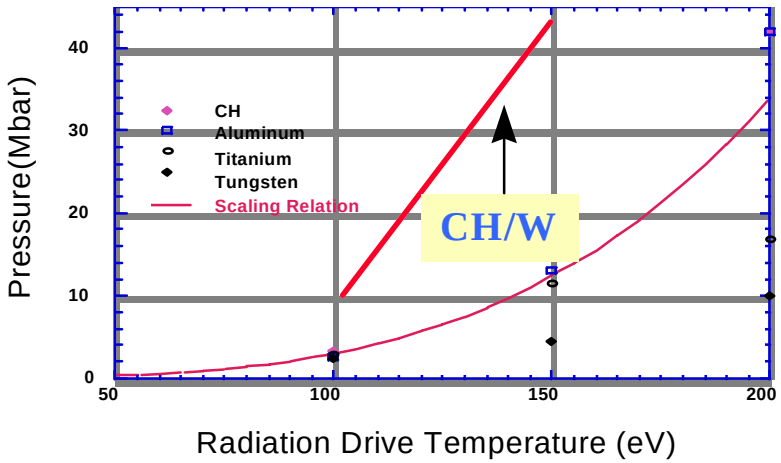

Figure 13. Pressures achievable with Z pinch sources as a function of radiation drive temperature.

4. Accomplishments

The following is a list of accomplishments.

- Computer Simulations: In an effort to optimize our dedicated equation-of-state (EOS) experiments, pressure profile simulations have been run to predict the capabilities of Z as a source to drive EOS experiments. In addition the codes have aided in identifying optimum target and Z drive configurations for dedicated EOS experiments which were conducted in early October.

- Instrumentation: Installation and interface into the Z environment of EOS instrumentation consisting of a Velocity Interferometer System for Any Reflector (VISAR) and associated equipment has been accomplished. This involved the following:

    1. Designing and fabricating a new miniature optical probe for VISAR measurements
    2. Characterization of the optical probe, Lithium Fluoride windows, and optical fibers for both fluorescence and optical darkening plus optical efficiency. Fluorescence and darkening are side effects of the Z environment and were tested both in the laboratory and at Z. This new probe design and fibers have been used on Z experiments.
    3. Unacceptable levels of noise were identified and localized to the laser required for VISAR experiments. A new laser configuration and addition of a screen box solved the problem.
    4. A VALYN VISAR system has been modified, removing three photomultiplier units (PMT's) and installation of fiber optics to couple the VISAR output to a streak camera.
    5. A fiber optic coupling cable with 30 data fibers has been designed and fabricated to interface the VISAR and shock breakout data to the streak camera.

6. A shock breakout system which records the change in reflectivity of a surface due to changes caused by a shock wave has been developed and tested in the laboratory.
7. Problems involving fluorescence of the breakout fibers caused by Z radiation overdriving the return data light have been resolved by the passing the return light through narrow (1nm) bandpass filters and increasing the input light energy through the use of a pulsed dye laser. We have been able increase the light energy coupled into the fiber optic splitter from 2 watts cw to kilowatt laser pulses.
8. The VISAR has been tested as "add-on" instrumentation to several existing experiments.

In summary, we are developing a new diagnostic using z pinch sources for producing high pressure shock waves. VISAR measurements of particle velocity and fiber optic measurements of particle velocity and shock speed are used for absolute EOS measurements. This report is a progress report on the development of this new technique, however, preliminary data obtained with the technique are encouraging.

5. References

1. Asay, J.R., and G.I. Kerley, *J., Impact Engng*,. **5**, 69 (1986).
2. Ragan, C.E., III, *Phys. Rev.* **A25**, 3360 (1982).
3. Evans, A.M., et al, *Laser and Particle Beams* **14**, 113 (1996).
4. Cauble, R., preprint, submitted to Physical Review Letters (1997).
5. Baumung, K., et al., *Laser and Particle Beams* **14**, 181 (1996).
6. Fortov, V., et al., *Shock Compression of Condensed Matter 1995,* Proceedings 370,Part 2,1255-1258,1995.
7. Olson, R.E., et al. Submitted to Phys. Plasmas, Volume 4, May1997
8. Barker, L. M., and Hollenbach, R.E., *J. Applied Physics*, Vol. 43, November 1972.
9. Budge, K.G. and Peery, J.S. *J. Impact Engng*.. **14**, 107-120 (1993).
10. Morel, J.E., Dendy, Jr., M.L., Hall, and S.W. White, Differencing Scheme, *Computational Physics* **103**, 286-299(19xx).
11. Morel, J.E., preprint (1997).
12. Dukart, R.J., Private communication (1997).

Distribution

Unclassified Unlimited Release

1	MS 9018	Central Technical Files, 8940-2
5	MS 0899	Technical Library, 4916
2	MS 0619	Review & Approval Desk, 12690 for DOE/OSTI
1	MS 1436	LDRD Office, 4523

Internal Distribution

1	MS0149	C. E. Meyers, 4000
1	MS0819	T. G. Trucano, 9231
1	MS0834	W. M. Trott, 9112
1	MS1168	M. D. Furnish, 9321
1	MS1181	J. R. Asay, 9575
1	MS1181	L. C. Chhabildas, 9575
1	MS1181	C. A. Hall, 9575
6	MS1181	C. H. Konrad, 9575
1	MS1182	D. D. Bloomquist, 9536
1	MS1184	D. L. Johnson, 9539
1	MS1186	D. L. Hanson, 9533
1	MS1187	R. E. Olson, 9571
1	MS1188	B. F. Clark, 9512
1	MS1193	J. Lash, 9531
1	MS1194	R. B. Spielman, 9573
1	MS1196	G. A. Chandler, 9577
1	MS1196	M. S. Derzon, 9577
1	MS1454	K. J. Fleming, 1554